Mon. Not. R. Astron. Soc. **000**, 000–000 (0000)   Printed 3 November 1998   (MN LATEX style file v1.4)

ROSAT HRI monitoring of extreme X-ray variability in the narrow-line quasar PHL 1092

W.N. Brandt,[1] Th. Boller,[2] A.C. Fabian[3] and M. Ruszkowski[3]

[1] *The Pennsylvania State University, 525 Davey Lab, University Park, PA 16802, USA*
[2] *Max-Planck-Institut für Extraterrestrische Physik, 85748 Garching, Germany*
[3] *Institute of Astronomy, Madingley Road, Cambridge CB3 0HA*

3 November 1998

ABSTRACT

We report results from an 18-day *ROSAT* HRI monitoring campaign on the ultrasoft Narrow-Line Seyfert 1 (NLS1) class quasar PHL 1092. This luminous, radio-quiet quasar showed strong X-ray variability in a short *ROSAT* PSPC observation, and *ROSAT* HRI monitoring of the similar object IRAS 13224–3809 revealed extreme variability on intermediate timescales. We wanted to determine whether remarkable X-ray variability persistently occurs in PHL 1092, and we also wanted to search for outstanding variability events that constrain emission processes. Given the large luminosity of PHL 1092 ($\sim 5 \times 10^{45}$ erg s^{-1} in the HRI band), we detect extremely rapid and large-amplitude X-ray variability throughout our monitoring. The maximum observed variability amplitude is a factor of ≈ 14, and in the most rapid variability event the HRI count rate increases by a factor of ≈ 3.8 in a rest-frame time interval of < 3580 s. The most rapid event has a rate change of luminosity of $> 1.3 \times 10^{42}$ erg s^{-2}, making it the most extreme such event we are aware of from a radio-quiet quasar. Standard 'radiative efficiency limit' arguments imply a radiative efficiency larger than can be achieved by accretion onto a Kerr black hole rotating at the maximum plausible rate, although we point out that such arguments depend upon the geometry of initial radiation release. Relativistic motions of the X-ray source are probably causing the radiative efficiency limit to break down; such relativistic motions have also been inferred in the similar NLS1-class quasar PKS 0558–504.

Key words: galaxies: individual: PHL 1092 – galaxies: active – X-rays: galaxies.

1 INTRODUCTION

PHL 1092 ($B = 16.7$; $z = 0.396$) is a luminous Narrow-Line Seyfert 1 (NLS1) class quasar that is one of the strongest optical Fe II emitters known (Bergeron & Kunth 1980). Such objects have been generally found to have extreme X-ray spectral and variability properties, and it appears likely that their exceptional X-ray/optical characteristics arise as the result of an extreme value of a primary physical parameter (see Brandt & Boller 1998 for a recent discussion). This primary parameter must ultimately originate from the immediate vicinity of the supermassive black hole since it can strongly influence the energetically-important and rapidly-variable X-ray emission.

The *ROSAT* PSPC spectrum of PHL 1092 is one of the softest ever seen from a quasar (Brandt 1995; Forster & Halpern 1996, hereafter FH96; Lawrence et al. 1996). For example, a simple power-law fit to the PSPC spectrum gives a photon index of $\Gamma = 4.2 \pm 0.5$. The poorly-sampled PSPC light curve showed remarkably rapid variability for such a luminous object. The count rate increased by a factor of ≈ 4 during a 2-day period, and there were weak indications for even more rapid variability. No strong spectral variability was apparent. FH96 used the 'radiative efficiency limit' of Fabian (1979) to argue that the implied radiative efficiency was $\eta > 0.13$, and they suggested that a Kerr black hole and/or anisotropic emission was implied. The other authors cited above interpreted the data in a somewhat more reserved manner (see below for discussion), and they found $\eta \gtrsim 0.02$. In this case, a Kerr black hole and/or anisotropic emission is not necessarily required.

We performed an 18-day *ROSAT* HRI monitoring campaign on PHL 1092 to further study its X-ray variability properties, and here we report the results from our campaign. Our monitoring goals were (1) to determine whether extreme X-ray variability persistently occurs in this quasar and (2) to search for outstanding variability events even

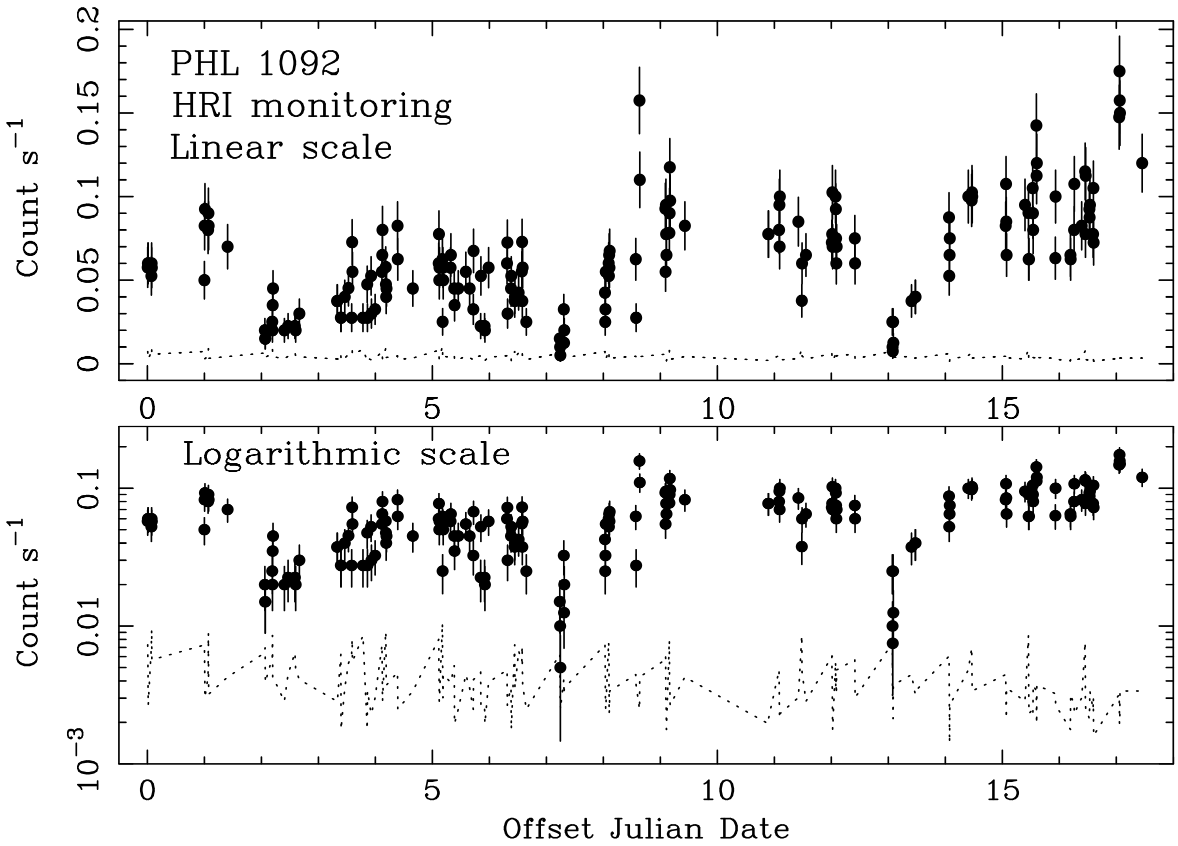

Figure 1. *ROSAT* HRI light curve for PHL 1092 obtained during the 18-day monitoring campaign between 1997 July 16 and 1997 August 2. The abscissa label gives the Julian date minus 2450645.12 days. The top panel shows the light curve with a linear ordinate, and the bottom panel shows the light curve with a logarithmic ordinate. Each data point is plotted at the middle of the 400 s exposure interval from which it was obtained, and the sizes of the exposure intervals lie within the data points themselves. The dashed curve indicates the background counting rate within the source extraction circle as a function of time.

more extreme than those seen by the PSPC. As we discuss below, goal 2 is important since such variability events can place constraints on emission processes and may elucidate the origin of the extreme properties of ultrasoft NLS1 more generally. This work builds upon our HRI monitoring of the similar but lower-luminosity ultrasoft NLS1 IRAS 13224–3809 (Boller et al. 1997, hereafter BBFF). PHL 1092 is ~ 40 times more luminous than IRAS 13224–3809.

The Galactic column density towards PHL 1092 is $(3.6 \pm 0.2) \times 10^{20}$ cm^{-2} (Murphy et al. 1996), and the PSPC spectrum constrained the intrinsic column density to be $< 2.0 \times 10^{20}$ cm^{-2}. We adopt $H_0 = 70$ km s^{-1} Mpc^{-1} and $q_0 = \frac{1}{2}$, and we hence derive a luminosity distance of 1840 Mpc. When we calculate luminosities below, we shall implicitly assume isotropic emission unless stated otherwise.

2 ROSAT HRI MONITORING RESULTS

2.1 Observations and spatial analysis

ROSAT HRI observations of PHL 1092 were performed between 1997 July 16 (02:47:15 UT) and 1997 August 2 (13:53:58 UT). The total exposure time was 109.135 ks, and the source was centred on-axis. Up to five separate observations were obtained each day, and coverage was reasonably good except for a period when PHL 1092 was not observable due the position of the Moon (the largest gap in Figure 1). All data analysis has been performed using FTOOLS.

We have added together all the HRI observations to produce a master image. The centroid position of PHL 1092 in the HRI master image is $\alpha_{2000} = 01^{\rm h}39^{\rm m}56.1^{\rm s}$, $\delta_{2000} = 06^\circ19'24.7''$. This position is in good agreement with the precise optical position given by Fanti et al. (1977), and there is no significant evidence for X-ray spatial extent after errors in attitude correction are taken into consideration (see Morse 1994). The source plus background photons at the HRI position of PHL 1092 were extracted using a circular source cell with a radius of 25 arcsec. The background was extracted using an annulus centred on PHL 1092 with an inner radius of 40 arcsec and an outer radius of 100 arcsec.

2.2 Count rate variability

In Figure 1 we show the full monitoring light curve for PHL 1092. Strong X-ray variability is apparent throughout the light curve. We have calculated the smallest and largest observed HRI count rates to determine the maximum variability amplitude. In such calculations, we always average over at least 4 of the data points shown in Figure 1 to prevent statistical count rate fluctuations from inducing artificially large variability amplitudes. The smallest count rate is observed between days 7.2–7.4 in Figure 1,

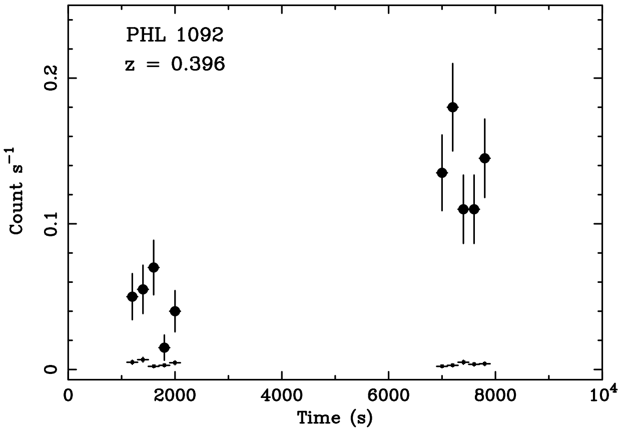

Figure 2. Light curve showing the most rapid observed variability during the HRI monitoring campaign. The HRI count rate for PHL 1092 is shown by the large circular data points, and the background count rate in the source cell is shown by the small square data points. The bin size is 200 s.

and the 6 data points during this span of time give a mean count rate of $(1.13 \pm 0.36) \times 10^{-2}$ count s^{-1}. The largest count rate is observed between days 17.0–17.2, and the 4 data points during this span of time give a mean count rate of $(1.57 \pm 0.16) \times 10^{-1}$ count s^{-1}. The most probable maximum variability amplitude is a factor of 13.9, and maximum variability amplitudes in the range 9.5–22.5 are most likely (Cauchy distributed; see section 2.3.4 of Eadie et al. 1971).

In Figure 2 we show the most rapid observed variability event. This event occurred around day 8.6 in Figure 1. The HRI count rate rose from $(3.46 \pm 0.98) \times 10^{-2}$ count s^{-1} to $(1.31 \pm 0.19) \times 10^{-1}$ count s^{-1}, thereby increasing by a factor of ≈ 3.8 in < 5000 s (< 3580 s in the rest frame of PHL 1092). We also detect 6 additional events where the HRI count rate exhibits a highly-significant increase or decrease by a factor > 2 in < 1 day.

2.3 Luminosity variability

We use the spectrum observed by the *ROSAT* PSPC to determine a conversion factor, f, between HRI count rate and luminosity. Unlike FH96, we do not simply extrapolate a steep ($\Gamma = 4.2$) power-law model down to 0.1 keV to derive a 0.1–2.0 keV luminosity. The extrapolation of a steep power-law spectrum to low energies where Galactic absorption is important can lead to unphysically large, or at least highly uncertain, luminosities. For such models most of the luminosity lies between 0.1–0.2 keV where few counts are actually detected.*

We have instead considered the luminosity from 0.2–2.0 keV in the observed frame since, for the Galactic column density relevant here, this quantity is much less dependent upon the details of the spectral model. We have considered three spectral models that give statistically acceptable fits to the PSPC data: a power-law model (M1), a power-law plus double blackbody model (M2) and a power-law plus bremsstrahlung model (M3). Using XSPEC (Arnaud 1996) and PIMMS (Mukai 1997), we find $f_{\rm M1} = 6.0 \times 10^{46}$ erg count^{-1}, $f_{\rm M2} = 4.8 \times 10^{46}$ erg count^{-1} and $f_{\rm M3} = 5.2 \times 10^{46}$ erg count^{-1}. In order to be reasonably conservative, we shall adopt $f_{\rm M2}$.

We find that the 0.2–2.0 keV luminosity of PHL 1092 varies between $(5.4 \pm 1.7) \times 10^{44}$ erg s^{-1} and $(7.5 \pm 0.8) \times 10^{45}$ erg s^{-1} during our monitoring observation. If we assume that the optical continuum is not highly variable on timescales of a few weeks (cf. section 3.1 of FH96), the $\alpha_{\rm ox}$ value for PHL 1092 varies between -1.8 and -1.4 (we calculate $\alpha_{\rm ox}$ between 3000 Å and 2 keV). For comparison, the $\alpha_{\rm ox}$ range for optically selected quasars is $\approx -1.5 \pm 0.1$ (e.g. Laor et al. 1997). For the variability event shown in Figure 2, we detect a change in HRI count rate of $(9.64 \pm 2.14) \times 10^{-2}$ count s^{-1}. This corresponds to a luminosity change of $\Delta L = (4.6 \pm 1.0) \times 10^{45}$ erg s^{-1} in a rest-frame time interval of $\Delta t < 3580$ s.

3 DISCUSSION

3.1 Radiative efficiency limit arguments

The variability event shown in Figure 2 has $\frac{\Delta L}{\Delta t} > 1.3 \times 10^{42}$ erg s^{-2}, making it the most extreme such event we are aware of from a radio-quiet quasar (compare with Remillard et al. 1991 and table 3 of FH96). This can be further quantified by employing the radiative efficiency (η) limit: $\eta > 4.8 \times 10^{-43} \frac{\Delta L}{\Delta t}$ (Fabian 1979). Straightforward application of the limit gives an extremely high $\eta > 0.62 \pm 0.13$. For comparison, optimal accretion onto a Kerr black hole rotating at the maximum plausible rate gives only $\eta \approx 0.3$ (see Thorne 1974).

The extreme radiative efficiency derived above provides motivation to critically examine the assumptions underlying the radiative efficiency limit. The standard derivation assumes that the radiation release associated with an observed luminosity outburst occurs entirely at the centre of the emission region. If the radiation release is more uniform, the rapid emission of photons from the outer few Thomson depths facing the observer can invalidate the standard derivation (see Appendix A). A rapid *rise* in the flux from a source, such as we have for PHL 1092 (and such as has been typically used in the literature), need not therefore involve the whole source and no limit applies.

We can, however, recover the situation if either (a) we assume restrictions upon the manner of radiation release or (b) we can place an upper limit upon the Thomson depth of the emission region. For case (a), we return to the original efficiency limit if all parts of the region emitting the sharp flux increase are in causal contact with each other (rather than with some remote centre of an idealized sphere; see Appendix A). For case (b), we have from Appendix A when $\tau_{\rm T}$ is large that $\Delta t = \vartheta \frac{h}{c} = \vartheta \frac{R}{\tau_{\rm T} c}$ where ϑ is a geometrical factor of order unity. Thus $\tau_{\rm T} = \vartheta \frac{R}{c \Delta t}$. If we can place an upper limit on R we also place an upper limit on $\tau_{\rm T}$. The emission dominating the *ROSAT* band is from the soft X-ray excess, and this emission is thought to be associated with the inner accretion disk. If we first make the assumption of blackbody emission we obtain $R < 4 \times 10^{11} L_{44}^{1/2} T_6^{-2}$ cm where L_{44} is the total blackbody luminosity in units of 10^{44} erg s^{-1} and

* This is the cause of the much higher radiative efficiency derived by FH96 as compared to Brandt (1995) and Lawrence et al. (1997).

T_6 is the blackbody temperature in units of 10^6 K. We have $L_{44} \approx 50$, and T_6 is unlikely to be smaller than $\approx$ 0.35 based on accretion disk theory and observations of the soft X-ray excess in similar objects (see equation 3.20 of Peterson 1997; measured soft X-ray excess temperatures are usually larger than this but will be strongly affected by relativistic effects if the black hole is Kerr). We then find $R \lesssim 2.3 \times 10^{13}$ cm and $\tau_{\rm T} \lesssim 0.5\vartheta$. While the derived R constraint is physically plausible (of order a couple gravitational radii for a black hole mass of $\approx 10^8$ $M_\odot$), the low Thomson depth is inconsistent with the assumption that $\tau_{\rm T}$ is large. Thus when the source size is determined by blackbody radiation, one cannot escape the efficiency limit by invoking large $\tau_{\rm T}$ as is done in Appendix A. Additional opacity sources, such as free-free absorption, are expected in the case of blackbody or quasi-blackbody emission. These have the effect of strengthening the above argument ($\tau_{\rm T}$ is replaced by an effective $\tau_{\rm Tot} > \tau_{\rm T}$ that includes the additional opacity sources).

Another possibility for case (b) is that the emission is due to Comptonization (which is plausibly the fastest emission process in this band). In this case, a cloud of gas bathed in soft photons is impulsively heated. The soft photons must originate at energies below the HRI band for large variability to be seen. Large spectral variations will occur as the outgoing photons are successively Compton upscattered before escaping unless the electron temperature is large and $\tau_{\rm T}$ is small (see Guilbert, Fabian & Ross 1982). The relative change in photon energy per scattering is $4kT/mc^2$, and therefore $kT \sim mc^2/4$ in order that many of the first burst of photons, which scatter at most once, appear in the HRI band. Such a high temperature requires that the Thomson depth of the whole source is small. The equilibrium Compton scattering formulae given by Zdziarski (1985; e.g. his equation 5; we correct his equation 6) require that $\tau_{\rm T} \sim 0.04$ if $kT/mc^2 \sim 0.25$ in order to obtain the steep mean photon index from the source of $\Gamma = 4.2 \pm 0.5$. Again this upper limit on $\tau_{\rm T}$ allows a lower bound to be placed upon η.

The precise value of the coefficient in the efficiency limit does depend upon geometry and can be uncertain by a factor of a few. We have seen that plausible constraints on radiation mechanisms make it unlikely that the much larger uncertainty theoretically possible for a large sphere is realised. We note further that there are likely to be inefficiencies in the conversion of the accretion energy into radiation, with some energy ending in kinetic or magnetic form. We conclude that the rapid variation seen in Figure 2 requires an efficiency of at least ≈ 0.10 and more probably ≈ 0.60.

3.2 Relativistic X-ray boosting in ultrasoft NLS1?

A straightforward application of the radiative efficiency limit to our most rapid observed variability implies $\eta > 0.62 \pm 0.13$. This appears to be substantially larger than can be explained without allowing for relativistic effects, but moderate relativistic boosting can easily explain our data (see Guilbert, Fabian & Rees 1983 and BBFF). The relativistic bulk motions required are of order $0.3c$ and might plausibly arise in the inner accretion disk. Relativistic X-ray boosting associated with a strong jet appears less likely given the spectral character of the soft X-ray emission and the fact that PHL 1092 is radio quiet.

Evidence for relativistic X-ray variability enhancement has been found in two other NLS1-class objects to date: PKS 0558–504 and IRAS 13224–3809. PKS 0558–504 showed a rapid X-ray flare that implied relativistic motions (Remillard et al. 1991), while IRAS 13224–3809 shows persistent, giant-amplitude, nonlinear variability that is most naturally explained via relativistic effects (BBFF). Our data on PHL 1092 now add further weight to the idea that unusually strong relativistic effects may be present in many ultrasoft NLS1. This hypothesis can be further examined by searching for X-ray spectral changes during putative relativistic variability events. *XMM* has the large collecting area and low-energy sensitivity needed for this work, and we hope to perform such observations.

ACKNOWLEDGMENTS

We thank the *ROSAT* team for scheduling help. ACF acknowledges support from the Royal Society. MR acknowledges support from an External Research Studentship of Trinity College, Cambridge; an ORS award; and the Stefan Batory Foundation. This work has been supported by NASA grant NAG5-6023 and a NASA LTSA grant.

REFERENCES

Arnaud K.A., 1996, in Jacoby G., Barnes J., eds, Astronomical Data Analysis Software and Systems V: ASP Conference Series # 101. ASP Press, San Francisco, p. 17
Bergeron J., Kunth D., 1980, A&A, 85, L11
Boller Th., Brandt W.N., Fabian A.C., Fink H., 1997, MNRAS, 289, 393 (BBFF)
Brandt W.N., 1995, PhD thesis, University of Cambridge
Brandt W.N., Boller Th., 1998, Astron. Nach., 319, 7 (Proc. of the Potsdam X-ray Surveys Workshop; astro-ph/9711158)
Eadie W.T., Drijard D., James F.E., Roos M., Sadoulet B., 1971, Statistical Methods in Experimental Physics. North-Holland, Amsterdam
Fabian A.C., 1979, Proc. Roy. Soc. London A, 366, 449
Fanti C., Fanti R., Lari C., Padrielli L., van der Laan H., de Ruiter H., 1977, A&A, 61, 487
Forster K., Halpern J.P., 1996, ApJ, 468, 565 (FH96)
Guilbert P.W., Fabian A.C., Ross R.R., 1982, MNRAS, 199, 763
Guilbert P.W., Fabian A.C., Rees M.J., 1983, MNRAS, 205, 593
Laor A., Fiore F., Elvis M., Wilkes B.J., McDowell J.C., 1997, ApJ, 477, 93
Lawrence A., Elvis M.S., Wilkes B.J., McHardy I., Brandt W.N., 1997, MNRAS, 285, 879
Morse J.A., 1994, PASP, 106, 675
Mukai K., 1997, PIMMS Users' Guide. NASA/GSFC, Greenbelt
Peterson B.M., 1997, An Introduction of Active Galactic Nuclei. Cambridge Univ. Press, Cambridge
Remillard R.A., Grossan B., Bradt H.V., Ohahsi T., Hayashida K., Makino F., Tanaka Y., 1991, Nature, 350, 589
Sunyaev R.A., Titarchuk L.G., 1980, A&A, 86, 121
Thorne K.S., 1974, ApJ, 191, 507
Zdziarski A.A., 1985, ApJ, 289, 514

APPENDIX A: DEPENDENCE OF THE RADIATIVE EFFICIENCY LIMIT UPON THE GEOMETRY OF RADIATION RELEASE

The radiative efficiency limit was derived by arguing that a radiatively-inefficient source must have such a high particle

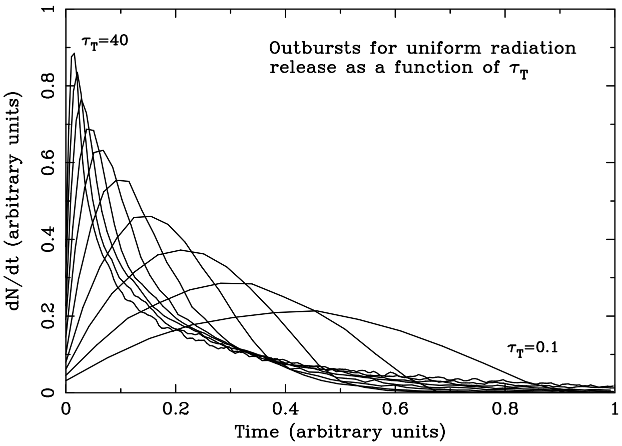

Figure A1. The photon flux detected at an observer $\frac{dN}{dt}$ versus time t for 10 logarithmically spaced values of $\tau_{\rm T}$ from $\tau_{\rm T} = 0.1$ to $\tau_{\rm T} = 40$. Smaller Thomson depths correspond to the curves with lower maximum values.

density that a rapid release of radiation in the source appears to an observer to be slowed down by Thomson scattering. For a luminosity outburst of amplitude ΔL with a rise time of Δt, the radiative efficiency η is defined by the equation

$$\Delta L \Delta t = \eta M c^2 \qquad \text{(A1)}$$

where M is the mass involved in the outburst and c is the speed of light. $M \approx m_{\rm p} n V$ where $m_{\rm p}$ is the mass of the proton, n is the proton number density (also assumed to be the electron number density), and V is the volume of the emission region. The standard derivation of the radiative efficiency limit (Fabian 1979) assumes a uniform, spherical emission region with the release of radiation localized at its centre, and it also assumes that relativistic Doppler boosting and light bending are unimportant. If the emission region has a significant Thomson depth ($\tau_{\rm T} \geq 1$), Δt must satisfy

$$\Delta t \geq (1+\tau_{\rm T})\frac{R}{c}, \qquad \tau_{\rm T} = n\sigma_{\rm T} R \qquad \text{(A2)}$$

where $\sigma_{\rm T}$ is the Thomson cross section and R is the radius of the region. The limit on η arises due to the competition between the light crossing time and the photon diffusion time. By combining equations (A1) and (A2) one obtains

$$\eta \geq \frac{\Delta L}{\Delta t} f(\tau_{\rm T}), \qquad f(\tau_{\rm T}) \propto \frac{(1+\tau_{\rm T})^2}{\tau_{\rm T}}. \qquad \text{(A3)}$$

$f(\tau_{\rm T})$ has the asymptotic behaviour

$$f(\tau_{\rm T}) \propto \begin{cases} \tau_{\rm T}^{-1} & \text{for } \tau_{\rm T} \ll 1 \text{ (light crossing time dominates)} \\ \tau_{\rm T} & \text{for } \tau_{\rm T} \gg 1 \text{ (photon diffusion time dominates).} \end{cases}$$

This means that there exists a minimum value of $f(\tau_{\rm T})$ (4 when $\tau_{\rm T} = 1$) and hence of η for a given ΔL and Δt.

In order to relax some of the assumptions entering the standard analytic derivation, we simulated photon diffusion from 'clouds' of moderate and high Thomson depths using Monte Carlo techniques. We first considered photon diffusion for the case described above with high Thomson depth and found our results to be consistent with the analytic results published by Sunyaev & Titarchuk (1980). We then considered a simple model of a uniform, spherical cloud but allowed radiation to be produced instantaneously throughout the cloud in a uniform manner. The results of the simulations for different Thomson depths are presented in Figure A1. The curves show the time dependence of the observed photon flux $\frac{dN}{dt} \propto L$ for a wide range of $\tau_{\rm T}$. There is an important difference in the behaviour of these curves as compared to the case when the radiation release occurs entirely at the centre of the cloud: when $\tau_{\rm T}$ becomes large there is now no reduction in the rate of increase of $\frac{dN}{dt}$ at the start of the outburst. In other words, at the start of the outburst $\frac{d^2N}{dt^2} \propto \frac{dL}{dt}$ increases monotonically as $\tau_{\rm T}$ is increased (even for $\tau_{\rm T} \gg 1$). This result can be understood by realizing that the radiation observed near the start of the outburst comes mostly from the outer few Thomson depths of the cloud facing the observer. The relevant 'cup-shaped' emission region at the start of the outburst is constrained by the surface of the cloud and the surface of equal photon arrival time. An upper limit to its volume for the diffusion dominated case is $V_{\rm cup} \leq \pi R^2 h$, where $h \approx \frac{R}{\tau_{\rm T}}$. Appropriate modification of equation (A3) leads to

$$\eta \geq \frac{\Delta L}{\Delta t}\tilde{f}(\tau_{\rm T}), \qquad \text{(A4)}$$

where

$$\tilde{f}(\tau_{\rm T}) \propto \tau_{\rm T}^{-2} \quad \text{for } \tau_{\rm T} \gg 1 \text{ (photon diffusion time dominates).}$$

The lower limit on the radiative efficiency in this case is a trivial $\eta \geq 0$.

The assumption that radiation is released instantaneously throughout the cloud is obviously an unrealistic one because it violates causality. To investigate the effect of causality, we considered a 'trigger signal' propagating outwards from the centre of the cloud with speed c. Radiation is released in a volume element of the cloud only after the trigger signal reaches it. Inclusion of this effect in the simulations does not change the general behaviour described above; at the start of the outburst, $\frac{d^2N}{dt^2}$ increases monotonically as $\tau_{\rm T}$ is increased. Again the only constraint on the radiative efficiency is the trivial $\eta \geq 0$.

A nonzero lower limit for η can be derived if one considers somewhat different definitions for ΔL and Δt. For example, one could define the characteristic variation timescale Δt as the time (measured from the observed start of the outburst) it takes for ≈ 90 per cent of the outburst photons reach the observer. Similarly ΔL could be defined as 90 per cent of the energy liberated in the outburst divided by Δt. There is a nonzero lower limit for η with the above definitions (this has been checked numerically). However, in order to reliably obtain an efficiency bound in this way one must be able to determine the overall profile of an outburst. In particular, one must be able to measure any decaying 'tail' with reasonably high precision. This is usually not possible due to observational constraints and the complexity of active galaxy light curves (e.g. outbursts often overlap each other).

In summary, the radiative efficiency limit is quite sensitive to the geometry of radiation release within the emission region. Without constraints on this geometry or the Thomson depth of the emission region, it is difficult to place meaningful constraints on η.